



# Thermodynamic measurement of La–Fe and Y–Fe alloys by multi-Knudsen cell mass spectrometry

Takashi Nagai\*, Woong-hee Han, Masafumi Maeda

Institute of Industrial Science, The University of Tokyo, 4-6-1 Komaba, Meguro-Ku, Tokyo 153-8505, Japan

## ARTICLE INFO

### Article history:

Received 22 June 2010

Received in revised form 20 July 2010

Accepted 20 July 2010

Available online 29 July 2010

### Keywords:

Thermodynamic properties

Activity

Iron–rare earth alloy

Knudsen cell mass spectrometry

## ABSTRACT

The activities of La and Fe in the La–Fe alloys, and those of Y and Fe in the Y–Fe alloys were determined by multi-Knudsen cell mass spectrometry. The activities of La and Fe in La–Fe alloys with La from 39.3 to 94.3 at% were determined at 1473–1623 K, measuring the ion currents of the vapor of La and Fe in equilibrium with La–Fe melts, and liquid +  $\gamma$ Fe. The activities of Y and Fe in Y–Fe alloys with Y from 15.1 to 87.8 at% were calculated at 1473–1573 K by measuring the ion currents of vapor in equilibrium with  $\text{Fe}_{17}\text{Y}_2 + \text{Fe}_{23}\text{Y}_6$ ,  $\text{Fe}_{23}\text{Y}_6 + \text{Fe}_3\text{Y}$ ,  $\text{Fe}_3\text{Y} + \text{liquid}$ , Y–Fe melts, and liquid +  $\alpha\text{Y}$ .

© 2010 Elsevier B.V. All rights reserved.

## 1. Introduction

Rare earth (RE) elements have been increasingly used in a wide range of advanced materials, including permanent magnets [1,2], hydrogen storage alloys [3,4] and luminescent materials [5,6]. In steelmaking industries, studies have been conducted on the use of RE metals as deoxidants [7,8] since they have stronger affinities for oxygen than conventional deoxidants. Although thermodynamic properties of intermetallic compounds and molten alloys in RE–Fe systems are required to use RE metals in high temperature processes of steelmaking, those available in the literature [8–10] remain limited, which seems to be related to experimental difficulties brought by the high reactivity of RE metals.

Fig. 1(a) shows the phase diagram of the La–Fe, [11] although partial mixing enthalpy in the liquid phase of La–Fe alloy [12] or the effect of deoxidation in liquid steel [8] were studied in the literature, activity in La–Fe alloy has not been yet examined. In the case of the Y–Fe system (Fig. 1(b) [11]), there are several intermetallic compounds,  $\text{Fe}_{17}\text{Y}_2$ ,  $\text{Fe}_{23}\text{Y}_6$ ,  $\text{Fe}_3\text{Y}$  and  $\text{Fe}_2\text{Y}$ . Subramanian and Smith [13] reported Gibbs energies of formation of these compounds, which were determined by electromotive force (EMF) measurements at low temperature (893–1271 K). The activities of Y derived from their data, however, involve a contradiction: there is a segment where the activity of Y decreases in spite of increasing Y compo-

sition. Research other than that by Subramanian and Smith [13] focused on partial mixing enthalpy in the liquid phase [14].

The thermodynamic measurement of alloys containing a RE metal by traditional methods is very difficult because of such metals' strong affinity with oxygen. Using Knudsen mass spectrometry, the authors were successful in measuring the vapor pressure of RE metals and those in the alloys [15,16]. In this study, the activities of La and Fe in the La–Fe system, and that of Y and Fe in the Y–Fe system were determined by multi-Knudsen mass spectrometry.

## 2. Experimental

### 2.1. Multi-Knudsen cell mass spectrometry

Knudsen cell mass spectrometry was developed as a method to measure vapor pressures of alloys and compounds. In this method, vapor pressure is monitored as ion current which is proportional to the pressure. The pressure,  $P_i$ , and ion current of  $i$ -species,  $I_i$ , measured by mass spectrometer are related through the following fundamental equation: [17]

$$P_i = b \frac{I_i}{\sigma_i} T \quad (1)$$

where  $T$ ,  $b$  and  $\sigma_i$  are the absolute temperature, device sensitivity constant and ionization cross-section of  $i$ -molecule, respectively.

Multi-Knudsen cells allow the measurement of ion currents of evaporated species from two or more substances under identical conditions in an experimental run: one substance is an experimental specimen and others are taken as reference substances, which is typically pure substance  $i$ . In this case, the constants,  $b$  and  $\sigma_i$ , can be regarded as equivalent for the substances, and thus activity of  $i$  in the specimen,  $a_i$ , can be deduced directly:

$$a_i = \frac{P_{i \text{ in alloy}}}{P_i^0} = \frac{I_{i \text{ in alloy}}}{I_i^0} \quad (2)$$

\* Corresponding author. Tel.: +81 3 5452 6298; fax: +81 3 5452 6299.  
E-mail address: [nagai@iis.u-tokyo.ac.jp](mailto:nagai@iis.u-tokyo.ac.jp) (T. Nagai).

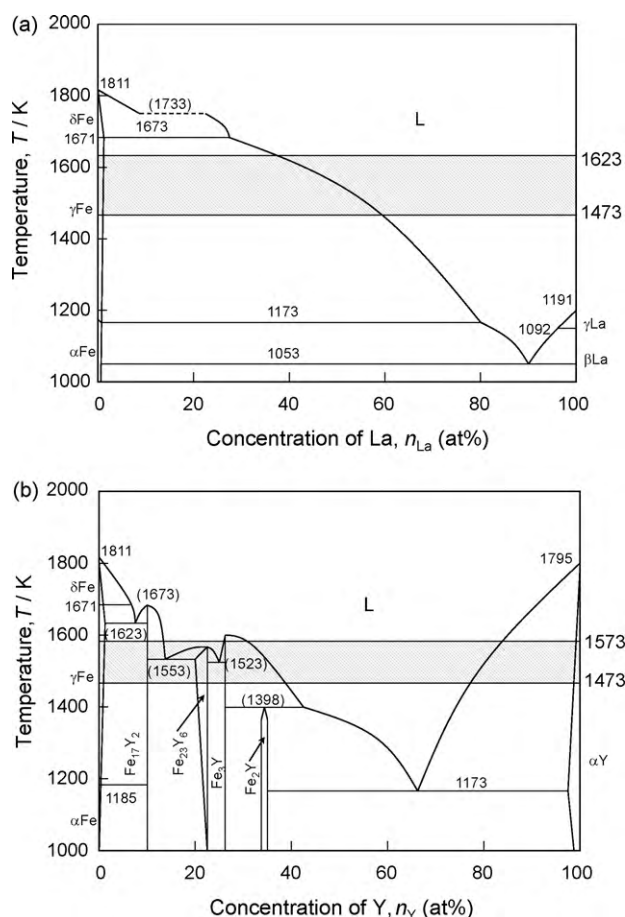


Fig. 1. Phase diagrams of binary systems, (a) La–Fe and (b) Y–Fe.

where  $P_i^0$  and  $I_i^0$  are the vapor pressure and the ion current of species  $i$  in equilibrium with the pure substance, respectively.

Details of the equipment for Knudsen cell mass spectrometry used in this study are described elsewhere [15–19]. A cell holder in a vacuum chamber could hold four Knudsen cells, and ion currents from each cell or background could be detected individually by rotating the cell holder. The cells were heated by a Ta electric resistance heating element. Temperatures of these cells were measured by three Pt–13% Rh/Pt thermocouples that were placed in holes drilled at the bottom of the cell holder. A quadrupole mass spectrometer (QMS) was used to monitor and measure ion currents of the evaporated species. The QMS was placed on top of the vacuum chamber in which the Knudsen cell unit was installed. The inside of the chamber was evacuated by a rotary pump and a turbo molecular pump (TMP), and the vacuum degree was kept below  $1.0 \times 10^{-4}$  Pa during experiments. The atomic or molecular beams of evaporated species from the Knudsen cell is injected into the ion source in QMS, where they are converted into positive ions by impact of the electrons emitted from the heated filament. Emission current of the filament and ionization potential were 2000  $\mu$ A and 102 eV, respectively. The ions in the ion source are injected into the quadrupole mass filter, which rejects all except those of a specific mass-to-charge ratio ( $m/z$ ); thereafter masses were detected by an electron multiplier.

La–Fe and Y–Fe master alloys were prepared by melting reagent grade La grain (99.99%) or reagent grade Y (99.9%) grain and electrolytic Fe (99.99%) with an electron beam melting technique. The alloys were melted three or four times, and were reversed up and down or crushed at each run. The compositions of the alloys were selected to be able to estimate the activities of La or Y and Fe at experimental temperature for any compositions based on the measured activities. The chemical compositions of the master alloys were determined by analysis with inductively coupled plasma atomic spectroscopy (ICP-AES, SPS4000, Seiko Instruments Inc.).

Reagent grade pure La grain (99.99%), Y grain (99.9%) and electrolytic Fe (99.99%) were used as a reference substance for the measurements of La–Fe and Y–Fe alloy. Since La and Y are easily oxidized in the air, the La and Y grains were preserved in spindle oil. They were put into a high vacuum chamber for measurement as soon as possible after being taken out of the oil and rinsed with acetone and ethanol within a short time. Before and after the experiment, the oxygen concentration of La and Y was analyzed by inert gas fusion-infrared absorptiometry (LECO N/O, TC-436AR), and the content was confirmed to be low enough to ignore.

Table 1

Conditions for activity measurements of Fe–La alloys.

Exp. #	Temperature, T/K	Concentration of La, (at%)	Phase
L1	1473–1623	$39.3 \pm 0.1$	( $\gamma$ Fe + liquid)
L2	1473–1623	$48.9 \pm 0.2$	(Liquid)
L3	1473–1573	$56.7 \pm 0.1$	(Liquid)
L4	1473–1598	$64.3 \pm 0.1$	(Liquid)
L5	1473–1573	$71.0 \pm 0.2$	(Liquid)
L6	1473–1573	$86.6 \pm 0.1$	(Liquid)
L7	1473–1573	$94.3 \pm 0.4$	(Liquid)

Table 2

Conditions for activity measurements of Fe–Y alloys.

Exp. #	Temperature, T/K	Concentration of Y, (at%)	Phase
Y1	1473–1573	$15.1 \pm 0.5$	( $\text{Fe}_{17}\text{Y}_2 + \text{Fe}_{23}\text{Y}_6$ ) – (liquid)
Y2	1473–1573	$23.2 \pm 0.1$	( $\text{Fe}_{23}\text{Y}_6 + \text{Fe}_3\text{Y}$ ) – (liquid)
Y3	1473–1573	$25.3 \pm 0.3$	( $\text{Fe}_3\text{Y} + \text{liquid}$ )
Y4	1473–1573	$49.1 \pm 0.3$	(Liquid)
Y5	1473–1573	$60.7 \pm 0.2$	(Liquid)
Y6	1473–1573	$70.2 \pm 0.4$	(Liquid)
Y7	1473–1573	$83.3 \pm 0.6$	( $\alpha\text{Y} + \text{liquid}$ ) – (liquid)
Y8	1473–1573	$87.8 \pm 0.2$	( $\alpha\text{Y} + \text{liquid}$ )

About 0.5 g of an experimental specimen, which was La–Fe or Y–Fe alloy, and reference specimens, which were pure La or Y and Fe, were charged to each Mo Knudsen cell with an inner crucible. The cells had a diameter of 10 mm, a height of 20 mm and thickness of 1 mm. The lid of each cell had an orifice; a lid with a 1.19 mm diameter orifice was used for measurements of La–Fe alloy and a lid with a 0.4 mm diameter orifice for Y–Fe alloy. According to Knudsen [20], the diameter of the orifice of a Knudsen cell must be less than one tenth of the mean free path of evaporated species so that Knudsen effusion is achieved. Mita et al. [21] by measuring the vapor pressure of zinc, detected that the ion current was proportional to partial pressure. The orifice of Knudsen cell in this study provided an equilibrium condition between gaseous and condensed phases at the experimental temperature. The materials of the inner crucibles were  $\text{Al}_2\text{O}_3$  for Fe, Mo for Y and Ta for La and the experimental alloys. As mentioned, the cell holder could hold four Knudsen cells. In each measurement, experimental alloy was charged to one of them, two references (La and Fe, or Y and Fe) were put into two cells and the fourth cell was empty to measure the ion current of the background.

The experimental conditions, i.e., temperature range, concentration of La in La–Y alloy, Y in Y–Fe alloy and measured phases are summarized in Tables 1 and 2.

### 3. Results and discussion

#### 3.1. La–Fe alloys

Ion currents from the La–Fe alloys, pure La and Fe were measured by multi-Knudsen cell mass spectrometry, representative results of these measurements are shown in Fig. 2. From the La–Fe alloys and pure La, ion currents were clearly detected at  $m/z = 139$ .

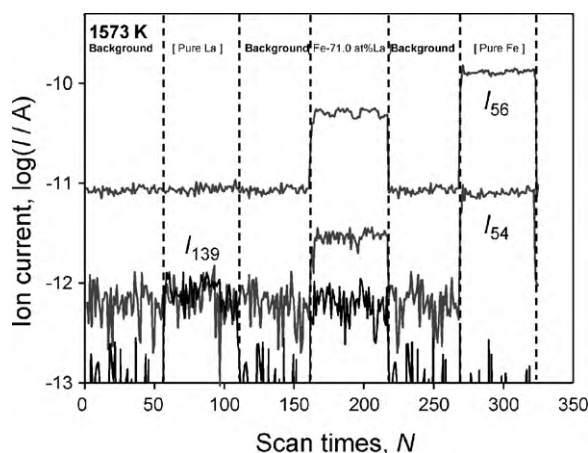


Fig. 2. Ion currents from La, Fe–La alloy and  $\gamma$ Fe.

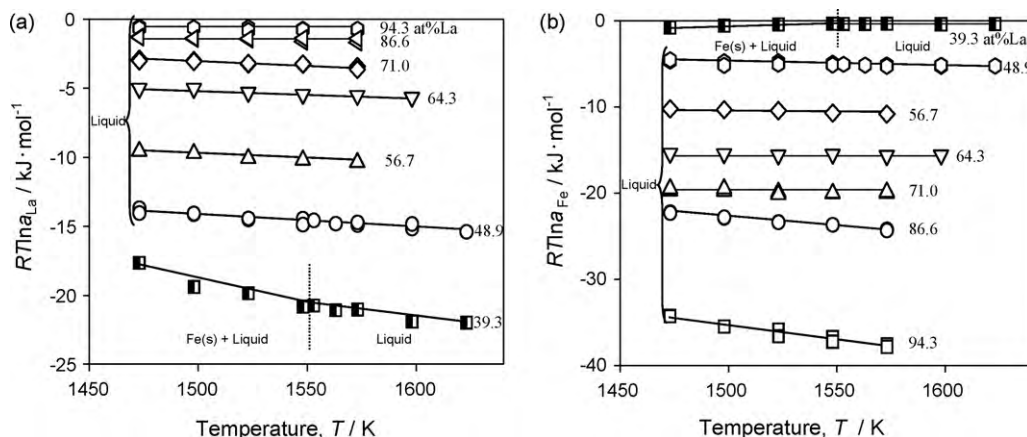


Fig. 3. Chemical potentials of La and Fe in La–Fe alloy, (a) La and (b) Fe.

This current would be due to  $^{139}\text{La}$ . La has isotopes of  $^{138}\text{La}$  and  $^{139}\text{La}$ , but no significant ion current was observed at  $m/z = 138$ , since the natural abundance of  $^{138}\text{La}$  is too low, 0.09% [22]. The ion current at  $m/z = 139$  was used for the derivation of the activity of La. From the La–Fe alloy and pure Fe, ion currents were detected at  $m/z = 54$  and 56. Fe has isotopes of  $^{54}\text{Fe}$ ,  $^{56}\text{Fe}$ ,  $^{57}\text{Fe}$ , and  $^{58}\text{Fe}$  [22], and their natural abundances are 5.8, 91.72, 2.2 and 0.28%, respectively. The ratio of the currents at  $m/z = 56$  and 54,  $I_{56}/I_{54} = 15.81$  for pure Fe and 15.92 for La–Fe alloy were in good agreement with that of the natural abundance of  $^{54}\text{Fe}$  and  $^{56}\text{Fe}$ ,  $^{54}\text{Fe}/^{56}\text{Fe} = 15.81$ , confirming that these currents were due to  $^{54}\text{Fe}$  and  $^{56}\text{Fe}$ . The ion currents due to  $^{57}\text{Fe}$  and  $^{58}\text{Fe}$  could not be detected because of their low natural abundance. The sum of the ion currents at  $m/z = 54$  and 56 was used as the ion current of Fe in the calculation of the activity.

As indicated by Eq. (2), the activities of La in the alloys can be determined as the proportion of ion current of La from the La–Fe alloy to that from pure La. The activity of Fe can also be obtained from the ion currents of Fe from the alloy and pure Fe. Fig. 3 shows the chemical potential ( $RT \ln a_{\text{La}}$  and  $RT \ln a_{\text{Fe}}$ ) against temperature. With increasing temperature, the chemical potential of each alloy except for that with 39.3 at% La slightly decreased linearly. Slopes of the lines for the alloy of 39.3 at% La changed at around 1550 K, since the phase of the alloy changes from solid Fe + liquid to a single liquid at this temperature. The liquidus line of the La–Fe system seems to be lower than that in the literature (Fig. 1(a)).

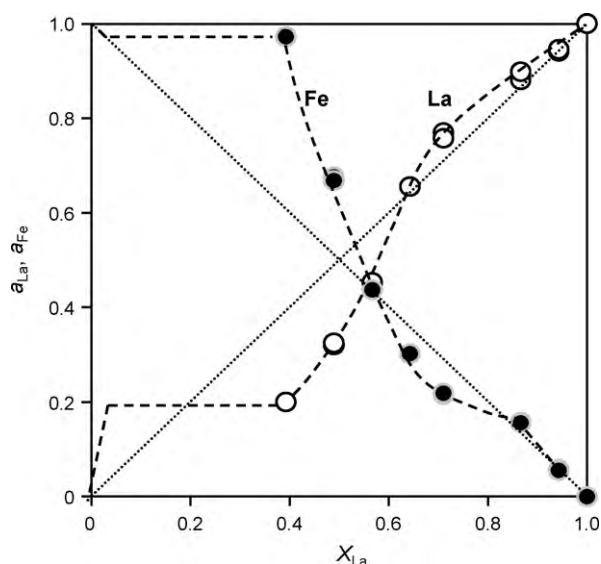


Fig. 4. Composition dependence of activities in La–Fe alloys at 1573 K.

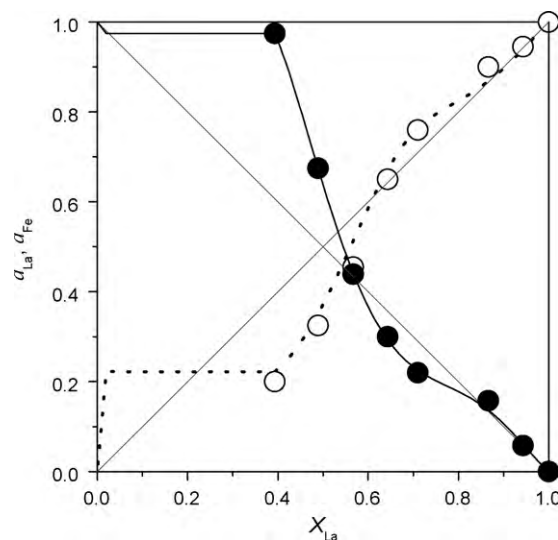


Fig. 5. Composition dependence of activities of La and Fe in La–Fe alloys at 1573 K. The activities of La and Fe determined by multi-Knudsen cell mass spectrometry are indicated by white and black marks, respectively. The dotted line shows La activity derived using the Gibbs–Duhem equation from the measured Fe activities.

The activities at 1573 K were replotted against the composition of the alloy in Fig. 4. The open and closed circles in the figure indicate the activities of La and Fe, respectively. Since the activities were measured in a wide range of composition, it is also possible to derive the activity of one component from that of the other one based on the Gibbs–Duhem equation. La activities were calculated from the

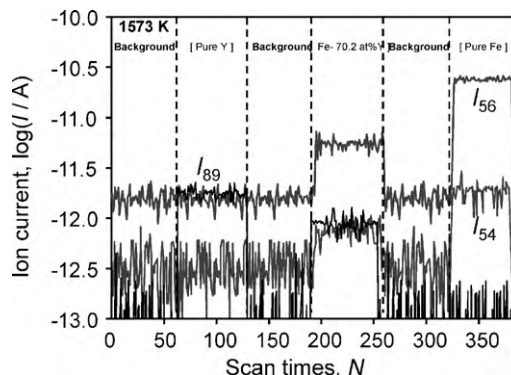


Fig. 6. Ion currents measured from  $\alpha\text{Y}$ , Fe–Y alloy and  $\gamma\text{Fe}$ .

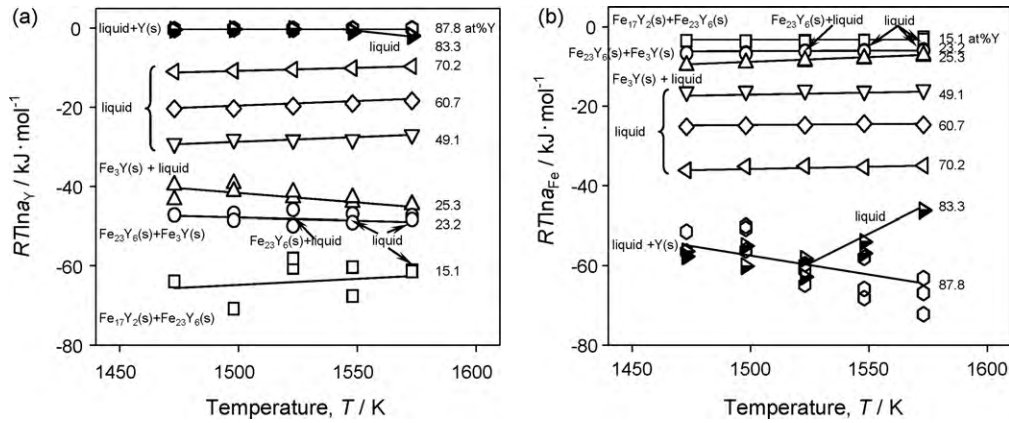


Fig. 7. Chemical potentials of Y and Fe in Y-Fe alloy, (a) Y and (b) Fe.

Fe activities using the following equation:

$$\ln \gamma_{\text{La}} = - \int_{X_{\text{Fe}}=1}^{X_{\text{Fe}}} \frac{X_{\text{Fe}}}{X_{\text{La}}} d \ln \gamma_{\text{Fe}} \quad (3)$$

where  $\gamma_i$  and  $X_i$  are the activity coefficient and mole fraction of  $i$  component, respectively. The derived La activity is shown in Fig. 5 by the dotted line, and it agreed well with the data directly measured by the multi-Knudsen cell mass spectrometry, this good agreement provides evidence that the activities were appropriately measured by multi-Knudsen cell mass spectrometry.

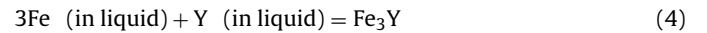
### 3.2. Y-Fe alloys

The multi-Knudsen cell mass spectrometry was carried out for the Y-Fe alloys using pure Y and Fe as reference substances. Fig. 6 shows ion currents measured from Fe-70.2 at% Y alloy, pure Y and pure Fe at 1573 K. From pure Y and the Y-Fe alloy, significant ion current was detected at  $m/z = 89$ . This current should be due to  $^{89}\text{Y}$ , since Y has no isotope other than  $^{89}\text{Y}$  [22]. Similar to the case of the La-Fe alloys, ion currents at  $m/z = 54$  and  $56$  were detected from the Y-Fe alloy and their ratio of  $I_{56}/I_{54} = 15.97$  was almost the same as the ratio of natural abundance of  $^{54}\text{Fe}$  and  $^{56}\text{Fe}$ , 15.81.

The activities of Y and Fe in the Y-Fe alloys were determined from the ion currents using Eq. (2), and the chemical potential against temperature of Y and Fe in these alloys is shown in Fig. 7. The

activities at 1473 and 1573 K are also plotted against mole fraction of Y in the alloy in Fig. 8.

From the measured activities of Fe and Y, the Gibbs energies of formations of  $\text{Fe}_3\text{Y}$ ,  $\Delta G_{\text{f Fe}_3\text{Y}}^\circ$ , were derived as follows.  $\Delta G_{\text{f Fe}_3\text{Y}}^\circ$  was calculated using the activities for the 25.3 at% Y-Fe alloy. The equilibrium reaction in this alloy can be expressed as Eq. (4), and there is a relationship between the chemical potential of component  $i$ ,  $\mu_i$ .



$$\mu_{\text{Fe}_3\text{Y}} = 3\mu_{\text{Fe}} + \mu_{\text{Y}} \quad (5)$$

Eq. (5) can be rewritten with  $\mu_i^\circ$ s and activities of  $i$  as follows:

$$\mu_{\text{Fe}_3\text{Y}}^\circ + RT \ln a_{\text{Fe}_3\text{Y}} = 3(\mu_{\text{Fe}}^\circ + RT \ln a_{\text{Fe}}) + \mu_{\text{Y}}^\circ + RT \ln a_{\text{Y}} \quad (6)$$

The activity of  $\text{Fe}_3\text{Y}$  is equal to unity since the compound is stoichiometric.

$$\mu_{\text{Fe}_3\text{Y}}^\circ - 3\mu_{\text{Fe}}^\circ - \mu_{\text{Y}}^\circ = 3RT \ln a_{\text{Fe}} + RT \ln a_{\text{Y}} \quad (7)$$

Therefore the following equation was derived,

$$\Delta G_{\text{f Fe}_3\text{Y}}^\circ = 3RT \ln a_{\text{Fe}} + RT \ln a_{\text{Y}} \quad (8)$$

Using the measured values  $a_{\text{Fe}}$  and  $a_{\text{Y}}$ ,  $\Delta G_{\text{f Fe}_3\text{Y}}^\circ$  was determined to be

$$\Delta G_{\text{f Fe}_3\text{Y}}^\circ = -119,000 + 34T \pm 20,000\text{J} \quad (9)$$

## 4. Conclusions

The activities of La and Fe in La-Fe alloys with La concentration from 39.3 to 94.3 at% were determined at 1473–1623 K by measuring the ion currents of the vapor of La and Fe in equilibrium with La-Fe melts and liquid +  $\gamma\text{Fe}$ .

The activities of Y and Fe in Y-Fe alloys with Y concentration from 15.1 to 87.8 at% were determined at 1473–1573 K by measuring the ion currents in equilibrium with  $\text{Fe}_{17}\text{Y}_2 + \text{Fe}_{23}\text{Y}_6$ ,  $\text{Fe}_{23}\text{Y}_6 + \text{Fe}_3\text{Y}$ ,  $\text{Fe}_3\text{Y} + \text{liquid}$ , Y-Fe melts and liquid +  $\alpha\text{Y}$ .

The Gibbs energies of formation of  $\text{Fe}_3\text{Y}$ ,  $\text{Fe}_{23}\text{Y}_6$ , and  $\text{Fe}_{17}\text{Y}_2$  were estimated with the activities of Y and Fe in Y-Fe alloy.

## Acknowledgements

The authors thank Professor Shu Yamaguchi in Department of Materials Engineering, School of Engineering, The University of Tokyo, for valuable discussion on chemical potentials;

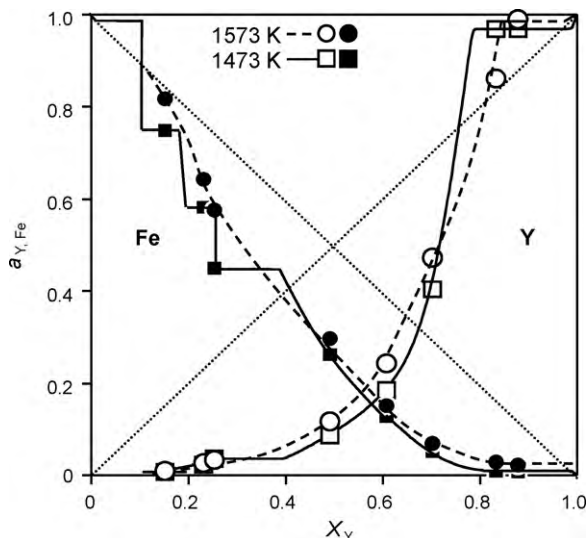


Fig. 8. Composition dependence of activities in Y-Fe at 1473 and 1573 K.



Professor Kazuki Morita and Professor Toru H. Okabe in Institute of Industrial Science, The University of Tokyo for helpful discussion; as well as Dr. Masao Miyake in Graduate School of Energy Science, Kyoto University for advice throughout this project.

## Appendix A.

The Gibbs energies of formation of  $\text{Fe}_{23}\text{Y}_6$  and  $\text{Fe}_{17}\text{Y}_2$ ,  $\Delta G_{\text{f Fe}_{23}\text{Y}_6}^\circ$  and  $\Delta G_{\text{f Fe}_{17}\text{Y}_2}^\circ$ , were also calculated with activities obtained in measurement of the 23.2 and 15.1 at% Y–Fe alloys. In this calculation, it was assumed that these compounds were stoichiometric and their activities could set at unity, although this was not true of  $\text{Fe}_{23}\text{Y}_6$ .

$\Delta G_{\text{f Fe}_{23}\text{Y}_6}^\circ$  was determined using the activities for the 23.2 at% Y–Fe alloy in which  $\text{Fe}_3\text{Y}$  and  $\text{Fe}_{23}\text{Y}_6$  are in equilibrium. The equilibrium can be expressed as



$$\Delta G_{\text{f Fe}_{23}\text{Y}_6}^\circ = 6\Delta G_{\text{f Fe}_3\text{Y}}^\circ + 5RT \ln a_{\text{Fe}} \quad (11)$$

Thus, by the above-obtained  $a_{\text{Fe}}$  and  $\Delta G_{\text{f Fe}_3\text{Y}}^\circ$ ,  $\Delta G_{\text{f Fe}_{23}\text{Y}_6}^\circ$  could be determined to be

$$\Delta G_{\text{f Fe}_{23}\text{Y}_6}^\circ = 459,000 + 14T \pm 360,000 \quad (12)$$

In the same manner,  $\Delta G_{\text{f Fe}_{17}\text{Y}_2}^\circ$  was obtained using the equilibrium in the 15.1 at% Y–Fe alloy. The equilibrium in this alloy can be expressed as



$$3\Delta G_{\text{f Fe}_{17}\text{Y}_2}^\circ = \Delta G_{\text{f Fe}_{23}\text{Y}_6}^\circ + 28RT \ln a_{\text{Fe}} \quad (14)$$

$\Delta G_{\text{f Fe}_{17}\text{Y}_2}^\circ$  could be determined to be

$$\Delta G_{\text{f Fe}_{17}\text{Y}_2}^\circ = 20,000 - 46T \pm 386,000 \quad (15)$$

$\Delta G_{\text{f Fe}_{23}\text{Y}_6}^\circ$  and  $\Delta G_{\text{f Fe}_{17}\text{Y}_2}^\circ$ , however, contain large errors because of the assumption and calculating methods.

## References

- [1] J.J. Croat, J.F. Herbst, R.W. Lee, F.E. Pinkerton, J. Appl. Phys. 55 (1984) 2078.
- [2] M. Sagawa, Mater. Jpn. 40 (2001) 934–946.
- [3] K.H.J. Buschow, in: K.A. Gschneidner Jr., L. Eyring (Eds.), Handbook on the Physics and Chemistry of Rare Earths, vol. 6, Elsevier, Amsterdam, 1984 (Chapter 47).
- [4] N. Sato, N. Morishita, T. Kimura, N. Fujioka, O. Takahishi, S. Bito, Y. Hattori, Y. Dansui, M. Ikoma, Matsushita Technol. J. 48 (2002) 15–20.
- [5] J.E. Geusic, H.M. Marcos, L.G. Van Uitert, Appl. Phys. Lett. 4 (1964) 182.
- [6] K. Ohno, T. Abe, J. Electrochem. Soc. 134 (1987) 2027.
- [7] T. Dan, K. Gunji, Tetsu-to-Hagane 14 (1) (1982) 915.
- [8] H. Nagai, Handbook on the Physics and Chemistry of Rare Earth 25 (1992) 1–49.
- [9] W.K. Lu, A. McLean, Ironmaking Steelmaking 1 (a) (1974) 228.
- [10] W.K. Lu, A. McLean, Met. Mater. (1974) 452.
- [11] T.B. Massalski (Ed.), Binary Alloy Phase Diagrams, ASM, Metal Park, OH, 1986.
- [12] V.V. Berezutskii, N.I. Usenko, M.I. Ivanov, Powder Metall. Met. Ceram. 45 (5–6) (2006) 266.
- [13] P.R. Subramanian, J.F. Smith, CALPHAD 8 (4) (1984) 295–305.
- [14] G.M. Ryss, A.I. Stroganov, Yu.O. Esin, P.V. Gel'd, Russ. J. Phys. Chem. 50 (3) (1976) 454–455.
- [15] W.H. Han, T. Nagai, M. Miyake, M. Maeda, Metall. Mater. Trans. 40 (5) (2009) 656–661.
- [16] W.H. Han, M. Miyake, T. Nagai, M. Maeda, J. Alloys Compd. 481 (2009) 241–245.
- [17] M. Heyrman, C. Chatillon, H. Collas, J. Chemin, Rapid Commun. Mass Spectrom. 18 (2004) 163–174.
- [18] T. Nagai, M. Miyake, Y. Mitsuda, H. Kimura, M. Maeda, ISIJ Int. 47 (2007) 207–210.
- [19] T. Nagai, M. Miyake, H. Kimura, M. Maeda, J. Chem. Thermodyn. 40 (2008) 471–475.
- [20] M. Knudsen, Annalen der Physik 28 (1909) 999.
- [21] K. Mita, S. Yamaguchi, M. Maeda, Met. Trans. B 35B (2004) 487–492.
- [22] R.L. David (Ed.), Handbook of Chemistry and Physics, 81st ed., 2000, pp. 1–15.